Nonreciprocity and Faraday Rotation at Time Interfaces

Huanan Li,[1,4,*] Shixiong Yin,[1,2,*] and Andrea Alù[1,2,3,†]
[1]Photonics Initiative, Advanced Science Research Center, City University of New York, New York, New York 10031, USA
[2]Department of Electrical Engineering, City College of The City University of New York, New York, New York 10031, USA
[3]Physics Program, Graduate Center, City University of New York, New York, New York 10016, USA
[4]School of Physics, Nankai University, Tianjin 300071, China

(Received 4 December 2021; accepted 4 April 2022; published 29 April 2022)

Nonreciprocity is critically important in modern wave technologies, yet its general principles and practical implementations continue to raise intense research interest, in particular in the context of broken reciprocity based on spatiotemporal modulation. Abrupt changes in time of the electromagnetic properties of a material have also been shown to replace spatial boundaries, supporting highly unusual wave-matter interactions in so-called time metamaterials. Here, we introduce nonreciprocity for temporal boundaries, demonstrating Faraday polarization rotation in a magnetoplasma with material properties abruptly switched in time. Our findings open new opportunities for time metamaterials, yielding new avenues for nonreciprocity with broad applicability for wave engineering.

DOI: 10.1103/PhysRevLett.128.173901

Since the devolvement of special relativity in the last century, space and time have been tightly connected in our understanding of the physical world. In metamaterials, modulation schemes exploiting the temporal degree of freedom have been providing a powerful framework to manipulate waves and realize new possibilities beyond static approaches [1]. As an important class, abrupt changes in time introducing temporal boundaries offer a simple and efficient way to break the limitations of time invariant materials, drawing increasing attention in recent years [2–15]. Intense research in this platform has proven fruitful, enabling intriguing phenomena like the inverse prism [16], temporal aiming [17], broadband absorption [18–20], unitary excitation transfer [21] and extreme energy transformations [22].

Lorentz reciprocity is a fundamental constraint for wave propagation in time-invariant linear systems described by symmetric constitutive tensors [23], requiring that the received signals are invariant when we swap the position in space of sources and detectors, leading to a symmetric scattering matrix. Breaking reciprocity is critical to realize devices like isolators and circulators, important for wireless communications and signal processing across a broad spectral range from microwave to optical frequencies. Usually, nonreciprocity can be achieved employing magneto-optical and/or nonlinear materials [24–31]. As an interesting alternative, spatiotemporal modulation as a tool to break reciprocity has generated significant interest in recent years [32–41]. By periodically modulating the material properties of a system in time with an asymmetric pattern in space, it is indeed possible to break degeneracies and time-reversal symmetry in various platforms, offering a viable alternative to magnetic bias and nonlinearities to realize nonreciprocal devices.

In this Letter, we connect the research interest in temporal boundaries and in nonreciprocity, and map the problem of nonreciprocity from the spatial to the temporal domain, studying the analog of nonreciprocal wave propagation for time interfaces. In particular, we study wave propagation with arbitrary polarization states in unbounded dispersive magnetoplasma media undergoing temporal discontinuities. To this end, we develop a general temporal transfer matrix framework, dual to its spatial equivalent, in which momentum rather than energy is conserved upon temporal switching. Based on this formalism, we extend the concept of nonreciprocity to time metamaterials, and explore the analogue of Faraday polarization rotation in a temporally switched unbounded medium. This approach may simplify the realization of nonreciprocal devices in various practical settings, eliminating the need to confine the wave or pattern structures in space.

Faraday polarization rotation.—One of the most classical nonreciprocal devices is the Faraday isolator, realized by sandwiching a 45° Faraday polarization rotator between two polarizers. Its functionality relies on the fact that the linear polarization of a wave is rotated nonreciprocally as it propagates in magneto-optical media, with a handedness that is a function of the applied magnetic bias and not of the direction of propagation. Dual to the concept we introduce in the following, we analyze this form of nonreciprocal polarization rotation through a standard scattering matrix formalism, for which the scattering matrix S in frequency domain relates the output ψ^o of the Faraday rotator to its input ψ^i as $\psi^o = S\psi^i$. Assuming input waves that propagate along the $\pm$z directions $\psi^i = [E_x^{L,i}, E_y^{L,i}, E_x^{R,i}, E_y^{R,i}]^T$, the outputs can be written as $\psi^o = [E_x^{L,o}, E_y^{L,o}, E_x^{R,o}, E_y^{R,o}]^T$ with the elements being the

electric field components along the x or y axis at the left (L) or right (R) ports, and the subscript T denotes the transpose operation. For a 45° Faraday rotator, the components of the scattering matrix S satisfy $S_{31} = S_{41}$ for forward waves, while $S_{13} = -S_{14}$ for backward incidence. Clearly, these two relationships cannot be simultaneously satisfied in a reciprocal structure, since $S \neq S^T$ [42]. In the following, we aim at introducing the analog of this response in a homogeneous medium with no spatial boundaries by using time interfaces.

Wave evolution in temporal magnetoplasma slabs.—One of the most common implementations of a Faraday rotator consists of a slab of magnetized plasma in the presence of a static magnetic field along the propagation direction. The relative permittivity tensor

$$\bar{\bar{\varepsilon}}_r = \begin{bmatrix} \varepsilon & ja & 0 \\ -ja & \varepsilon & 0 \\ 0 & 0 & \varepsilon_z \end{bmatrix},$$

with elements following a Drude dispersion $\varepsilon = 1 + [\omega_p^2/\omega^2(1 - j\gamma/\omega)]/[\omega_c^2/\omega^2 - (1 - j\gamma/\omega)^2]$, $a = (\omega_p^2\omega_c/\omega^3)/[\omega_c^2/\omega^2 - (1 - j\gamma/\omega)^2]$, and $\varepsilon_z = 1 - (\omega_p^2/\omega^2)/(1 - j\gamma/\omega)$ under an $e^{j\omega t}$ time dependence [43], where ω_p is the plasma frequency, $\gamma > 0$ is the collision frequency, and the cyclotron frequency $\omega_c > 0$ is proportional to the static magnetic field $\vec{H}_{dc}$ pointing along $+z$. The medium supports ordinary and extraordinary waves along the z axis, with dispersion $k_z = n^+(\omega)\omega/c_0$ and $k_z = n^-(\omega)\omega/c_0$ respectively, where $n^\pm(\omega) = \sqrt{\varepsilon \mp a}$ is the equivalent refractive index and $c_0 = 1/\sqrt{\mu_0\epsilon_0}$ [with $\mu_0(\epsilon_0)$ being the vacuum permeability (permittivity)] is the speed of light in free space. The difference between $n^\pm$ determines the circular birefringence, which controls the degree of polarization rotation per unit length.

We consider here the time analog of a Faraday rotator, in which the spatial boundaries of a magnetoplasma slab are replaced by temporal interfaces obtained by abruptly switching its material parameters. Here we neglect nonlinearities and hysteresis arising in magneto-optical materials for large field variations, as we deal with small amplitude signals [44,45]. At each time interface the signal frequency changes but the wave number k_z is conserved. We assume that the incident wave prior to the switching events has $k_z \in \mathcal{R}$, hence its angular frequency ω generally takes complex values when γ is nonzero. Associated with each wave number k_z, a material characterized by our Drude $\bar{\bar{\varepsilon}}_r$ supports three pairs of complex-valued angular frequencies, denoted by $\omega_l^\pm$, $l = 1, 2, 3$ (with $\pm$ indicating the ordinary or extraordinary waves), obeying $\omega_2^+ = -(\omega_2^-)^*$ and $\omega_3^\pm = -(\omega_1^\mp)^*$ with $*$ indicating the complex conjugate operation [46]. Correspondingly, the eigenvectors for forward waves can be compactly written as

$$\begin{bmatrix} E_x \\ E_y \\ \eta_0 H_x \\ \eta_0 H_y \end{bmatrix} = \begin{bmatrix} 1, & 1, & 1 \\ j, & -j, & -j \\ -jn_1^+, & jn_1^-, & jn_2^- \\ n_1^+, & n_1^-, & n_2^- \end{bmatrix} \begin{bmatrix} f_1^+(t) \\ f_1^-(t) \\ f_2^-(t) \end{bmatrix} e^{-jk_z z} + \text{c.c.} \tag{1}$$

with $E_{x,y}$ ($H_{x,y}$) being the electric (magnetic) field components and $\eta_0 = \sqrt{\mu_0/\epsilon_0}$ being the characteristic impedance of free space [46], where $f_l^\pm(t) \propto e^{j\omega_l^\pm t}$ are the time-dependent amplitudes of forward waves, and $n_l^\pm \equiv n^\pm(\omega_l^\pm) = k_z c_0/\omega_l^\pm$ are their refractive indices. Similarly, for the backward waves

$$\begin{bmatrix} E_x \\ E_y \\ \eta_0 H_x \\ \eta_0 H_y \end{bmatrix} = \begin{bmatrix} 1, & 1, & 1 \\ -j, & j, & j \\ -j(n_1^+)^*, & j(n_1^-)^*, & j(n_2^-)^* \\ -(n_1^+)^*, & -(n_1^-)^*, & -(n_2^-)^* \end{bmatrix} \begin{bmatrix} b_1^+(t) \\ b_1^-(t) \\ b_2^-(t) \end{bmatrix} \times e^{-jk_z z} + \text{c.c.} \tag{2}$$

with time-dependent amplitudes $b_l^\pm(t) \propto e^{-j(\omega_l^\pm)^* t}$ [46]. In Fig. 1(a), we consider a lossless magnetoplasma and plot $\omega_l^\pm$ of the three forward waves versus the cyclotron frequency ω_c for $\omega_p = 0.8k_z c_0$ (solid lines) and $\omega_p = 0.535k_z c_0$ (dashed lines). When ω_c approaches to zero, one of the modes approaches zero frequency $\omega_2^- \to 0$, supporting the helical wiggler phenomenon [47].

Upon a temporal switching event, the incident wave can be coupled to all six modes with the same longitudinal momentum, and in order to evaluate their coupling suitable temporal boundary conditions are required. They can be derived considering Maxwell's equations in a time-varying magnetoplasma, supplemented by the continuity equation of the electrical charge and the dynamical equation for the plasma current density $\vec{J}$,

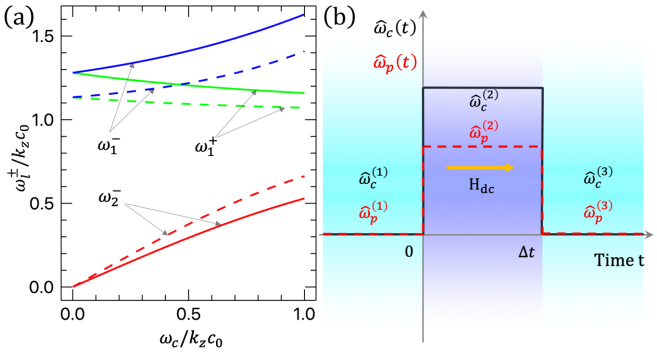

FIG. 1. (a) Angular frequencies $\omega_l^\pm$ (in units of $k_z c_0$) of forward waves in a magnetoplasma as a function of ω_c (in units of $k_z c_0$) when $\omega_p = 0.8k_z c_0$ (solid lines) and $\omega_p = 0.535k_z c_0$ (dashed lines). (b) Schematic of a temporal magnetoplasma slab.

$$\frac{\partial \vec{J}}{\partial t} + [\gamma - \omega_c(t)\hat{z}\times]\vec{J} = \epsilon_0 \omega_p^2(t)\vec{E}, \tag{3}$$

where both the cyclotron frequency $\omega_c(t)$ and the plasma frequency $\omega_p(t)$ may be discontinuous at a time boundary, and $\hat{z}$ denotes the unit vector. Using the method of distribution balance [48], the physical quantities $\vec{E}$, $\vec{H}$, and $\vec{J}$ are expected to be continuous across the time interface. These temporal boundary conditions are consistent with the results based on Laplace transform [49–52].

We proceed to investigate the wave evolution in temporal magnetoplasma slabs involving a series of switching events, in which we assume that both ω_c and ω_p may be abruptly changed [see, for example, Fig. 1(b)]. Using Eq. (3), the nonzero components of the current density $\vec{J}$ can be written as

$$\frac{1}{\epsilon_0}\begin{bmatrix} J_x \\ J_y \end{bmatrix} = \begin{bmatrix} \chi_1^+ j\omega_1^+, & \chi_1^- j\omega_1^-, & \chi_2^- j\omega_2^- \\ -\chi_1^+\omega_1^+, & \chi_1^-\omega_1^-, & \chi_2^-\omega_2^- \end{bmatrix} \begin{bmatrix} f_1^+(t) \\ f_1^-(t) \\ f_2^-(t) \end{bmatrix} \times e^{-jk_z z} + \text{c.c.} \tag{4}$$

for forward waves and

$$\frac{1}{\epsilon_0}\begin{bmatrix} J_x \\ J_y \end{bmatrix} = \begin{bmatrix} (\chi_1^+)^*(j\omega_1^+)^*, & (\chi_1^-)^*(j\omega_1^-)^*, & (\chi_2^-)^*(j\omega_2^-)^* \\ -(\chi_1^+)^*(\omega_1^+)^*, & (\chi_1^-)^*(\omega_1^-)^*, & (\chi_2^-)^*(\omega_2^-)^* \end{bmatrix} \times \begin{bmatrix} b_1^+(t) \\ b_1^-(t) \\ b_2^-(t) \end{bmatrix} e^{-jk_z z} + \text{c.c.} \tag{5}$$

for backward waves, where $\chi_l^\pm \equiv (n_l^\pm)^2 - 1$ is the effective electric susceptibility [46]. For one set of waves $s_1 = \{f_1^+(t), b_1^-(t), b_2^-(t)\}$, the complex-amplitude ratios of the y to x component of the electric field $\vec{E}$, the magnetic field $\vec{H}$, and the current density $\vec{J}$ are equal to j, while they are $-j$ for the other set $s_2 = \{b_1^+(t), f_1^-(t), f_2^-(t)\}$, indicating opposite polarization handedness of the supported eigenmodes, as expected due to the circular birefringence of the material. These two sets of eigenmodes are orthogonal to each other [46]. Consider, for instance, the first set s_1 with state vector $\psi_E^{s1}(t) \equiv [f_1^+(t), b_1^-(t), b_2^-(t)]^T$. At switching time t_s, the temporal boundary conditions together with Eqs. (1), (2), (4), (5) yield the simple relationship $\psi_E^{s1}(t_s^+) = J_{2,1}^{s1}\psi_E^{s1}(t_s^-)$ for the instantaneous variation of $\psi_E^{s1}(t)$, with matching matrix

$$J_{2,1}^{s1} = (A_{s1}^{(2)})^{-1}A_{s1}^{(1)}, \qquad A_{s1} \equiv \begin{bmatrix} 1 & 1 & 1 \\ -jn_1^+ & j(n_1^-)^* & j(n_2^-)^* \\ \chi_1^+ j\omega_1^+ & (\chi_1^-)^*(j\omega_1^-)^* & (\chi_2^-)^*(j\omega_2^-)^* \end{bmatrix}, \tag{6}$$

where the superscript of $A_{s1}^{(m)}$ refers to the material properties $m = 1, 2$ before and after switching. The evolution of the state vector $\psi_E^{s1}(t)$ in each temporal slab within medium m is described by $\psi_E^{s1}(t_2) = F_m^{s1}(t_2 - t_1)\psi_E^{s1}(t_1)$ through the diagonal propagation matrix

$$F_m^{s1}(\Delta t) = \text{diag}\{e^{j\omega_1^+\Delta t}, e^{-j(\omega_1^-)^*\Delta t}, e^{-j(\omega_2^-)^*\Delta t}\}. \tag{7}$$

The total transfer matrix M_{tot}^{s1}, accounting for the evolution of $\psi_E^{s1}(t)$ across a series of temporal interfaces, can be readily obtained from the cascade of J and F matrices. Similarly, we can construct the total transfer matrix M_{tot}^{s2} for the full evolution of the state vector $\psi_E^{s2}(t) \equiv [b_1^+(t), f_1^-(t), f_2^-(t)]^T$ for the wave set s_2. Given their relation, the total transfer matrix obeys $M_{\text{tot}}^{s2} = (M_{\text{tot}}^{s1})^*$, since $J_{2,1}^{s2} = (J_{2,1}^{s1})^*$ and $F_m^{s2}(\Delta t) = [F_m^{s1}(\Delta t)]^*$.

Now we are ready to investigate the wave evolution at a time interface. We assume excitation with a circularly polarized wave with incident frequency $\omega_{\text{inc}}(= k_z c_0) = 2\pi \times 1$ GHz in free space for a typical microwave experiment [49], i.e., $f_1^+(0^-) = 1$ and $b_1^-(0^-) = b_2^-(0^-) = 0$ for s_1, and assume that the magnetic bias is abruptly switched on at time $t = 0$, such that the wave travels in a magnetoplasma with normalized cyclotron frequency $\hat{\omega}_c \equiv \omega_c/\omega_{\text{inc}} = 0.5$ and normalized plasma frequency $\hat{\omega}_p \equiv \omega_p/\omega_{\text{inc}} = 0.8$. To avoid numerical issues associated with $\omega_2^- = 0$ in free space [see Fig. 1(a)], we describe free space before the switching event as a magnetoplasma with $\hat{\omega}_p = 10^{-5}$ and $\hat{\omega}_c = 0$, and add a small uniform loss $\gamma = 10^{-5}\omega_{\text{inc}}$ in both media. As shown in Fig. 2(a), the theoretical results (solid lines) match FDTD simulations carried assuming a long finite wave pulse (symbols), and $\vec{E}$, $\vec{H}$, and $\vec{J}$ are indeed continuous at $t = 0$. After a sufficiently long time, the finite forward and backward wave trains traveling at different velocities are separated in space in our FDTD simulations [53,54]; see Fig. 2(b) for a snapshot at time $t = 33.46T_{\text{inc}}$ (with $T_{\text{inc}} \equiv 2\pi/\omega_{\text{inc}}$) and the Supplemental Material [46] for a full animation.

In the case of excitation with arbitrary polarization states, we need to consider the full time-dependent state vector $\psi_E(t) \equiv \begin{bmatrix} \psi_E^{s1}(t) \\ \psi_E^{s2}(t) \end{bmatrix}$, which can be used to determine the total electric and magnetic fields with Eqs. (1)–(2) and the total current density $\vec{J}$ with Eqs. (4)–(5). The evolution of $\psi_E(t)$ across multiple temporal slabs is described by the total transfer matrix M_{tot},

$$\psi_E(t_f) = M_{\text{tot}}\psi_E(t_i), \qquad M_{\text{tot}} = \begin{bmatrix} M_{\text{tot}}^{s1} & 0 \\ 0 & (M_{\text{tot}}^{s1})^* \end{bmatrix}, \tag{8}$$

where t_f and t_i are the final and initial observation times.

Nonreciprocity in temporal slabs.—We are now ready to investigate the analog of Faraday rotation in temporal slabs.

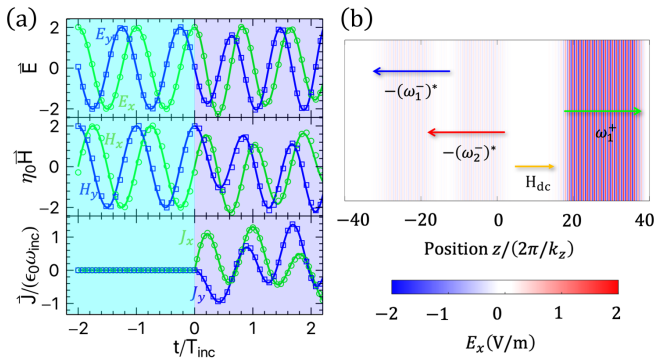

FIG. 2. (a) Time-dependent evolution of the nonzero components (in units of V/m) of the electric field $\vec{E}$, normalized magnetic field $\eta_0\vec{H}$ and plasma current density $\vec{J}/(\epsilon_0\omega_{\rm inc})$ at $z=0$ in the case of excitation with a circularly polarized wave propagating in a medium that switches abruptly at time $t=0$ from free space to a magnetoplasma with $\hat{\omega}_p=0.8$, $\hat{\omega}_c=0.5$ [see colored backgrounds]. Analytical and FDTD results are indicated by solid lines and symbols, respectively. (b) Snapshot of FDTD simulations for $E_x(z,t)$ versus z (in units of $2\pi/k_z$) at $t=33.46T_{\rm inc}$, when one forward wave (green arrow) and two backward waves (blue and red arrows) are clearly seen. Throughout our study, a small uniform time-independent loss $\gamma=10^{-5}\omega_{\rm inc}$ is assumed, and $\omega_{\rm inc}/(2\pi)=1$ GHz.

To this end, we consider the switching protocol shown in Fig. 1(b), for which the medium switches abruptly from free space to a magnetized plasma at time $t=0$, and then back to free space at time $t=\Delta t$. By employing Eq. (8), we obtain $M_{\rm tot}$ for the evolution of $\psi_E(t)$ from the initial time $t_i=0^-$ to the final time $t_f=\Delta t^+$, where the critical submatrix $M_{\rm tot}^{s1}$ reads

$$M_{\rm tot}^{s1}=J_{3,2}^{s1}F_2^{s1}(\Delta t)J_{2,1}^{s1}, \tag{9}$$

consisting of the matching matrices $J_{m+1,m}$, $m=1,2$ between subsequent media and the propagation matrix $F_2^{s1}(\Delta t)$ in medium $m=2$ for s_1, see Eqs. (6)–(7). To facilitate the analysis of temporal Faraday rotation, we construct the complex time-dependent amplitudes $E_x^f(t)$, $E_y^f(t)$ $[E_x^b(t),E_y^b(t)]$ for the electric field components E_x and E_y of forward [backward] waves from the elements of $\psi_E(t)$. Based on Eqs. (1)–(2),

$$\begin{bmatrix}E_x^f(t)\\E_y^f(t)\end{bmatrix}=\begin{bmatrix}1&1\\j&-j\end{bmatrix}\begin{bmatrix}f_1^+(t)\\f_1^-(t)\end{bmatrix},$$
$$\begin{bmatrix}E_x^b(t)\\E_y^b(t)\end{bmatrix}=\begin{bmatrix}1&1\\-j&j\end{bmatrix}\begin{bmatrix}b_1^+(t)\\b_1^-(t)\end{bmatrix}, \tag{10}$$

noting that in free space $f_2^-(t)$ and $b_2^-(t)$ are static fields with zero frequency, hence they do not contribute to the wave response. We can then introduce the temporal transmission coefficients $t_{L\to R}$ and $t_{R\to L}$, describing the transmission through the temporal slab for excitation from left and right, respectively, defined as

$$\begin{bmatrix}E_x^f(t_f)\\E_y^f(t_f)\end{bmatrix}=t_{L\to R}\begin{bmatrix}E_x^f(t_i)\\E_y^f(t_i)\end{bmatrix},\qquad \begin{bmatrix}E_x^b(t_f)\\E_y^b(t_f)\end{bmatrix}=t_{R\to L}\begin{bmatrix}E_x^b(t_i)\\E_y^b(t_i)\end{bmatrix}. \tag{11}$$

Reciprocity for time interfaces is defined as

$$t_{L\to R}=(t_{R\to L}^*)^T, \tag{12}$$

where the appearance of the complex conjugate is due to our definition of time-dependent amplitudes in Eq. (10) [see also Eqs. (1) and (2)] as compared with standard phasors for sinusoidal electromagnetic waves [55]. We point out that Eq. (12) is the generalization of the reciprocity condition for time interfaces, and it is indeed satisfied by all scenarios discussed in the recent literature on time metamaterials, e.g., in Ref. [11] where medium 2 in Fig. 1(b) is replaced by a dispersionless anisotropic medium with diagonal constitutive tensors. Indeed, it is easy to prove, based on our general formulation, that if the temporal slab involves reciprocal media with symmetric constitutive tensors, Eq. (12) is necessarily satisfied.

A 45° Faraday polarization rotation, ideally suited to realize isolation in the spatial scenario, requires the temporal transmission coefficients to obey the equalities $t_{L\to R}(1,1)=t_{L\to R}(2,1)$ and $t_{R\to L}^*(1,1)=-t_{R\to L}^*(1,2)$, evidently violating Eq. (12) and breaking temporal reciprocity. For the temporal slab in Fig. 1(b), the second equality follows from the first one since, based on Eqs. (8), (10), (11), the temporal transmission coefficients obey $t_{R\to L}=t_{L\to R}^*$ and the matrix elements of $t_{L\to R}$ read

$$t_{L\to R}(1,1)=t_{L\to R}(2,2)=\{M_{\rm tot}^{s1}(1,1)+[M_{\rm tot}^{s1}(2,2)]^*\}/2, \tag{13a}$$

$$t_{L\to R}(2,1)=-t_{L\to R}(1,2)=j\{M_{\rm tot}^{s1}(1,1)-[M_{\rm tot}^{s1}(2,2)]^*\}/2 \tag{13b}$$

with the matrix elements of $M_{\rm tot}^{s1}$ given in Eq. (9). Consequently, 45° temporal Faraday rotation is achieved when the figure of merit $\Delta\equiv|t_{L\to R}(1,1)-t_{L\to R}(2,1)|^2$ approaches zero.

In Fig. 3(a), we set $\hat{\omega}_c=0.7$, and show the dependence of $\log_{10}\Delta$ versus $\hat{\omega}_p$ and thickness Δt of the temporal slab [see Fig. 1(b)]. Choosing $\hat{\omega}_p\approx0.535$ and $\Delta t\approx1.28T_{\rm inc}$ we obtain $\Delta\approx0$, yielding an optimal point for perfect 45° polarization rotation [56]. Indeed, as shown in Fig. 3(b) (see also the Supplemental Material [46] for the corresponding Lissajous animation), a horizontally polarized wave, i.e., $E_y=0$, is converted into a linearly polarized one

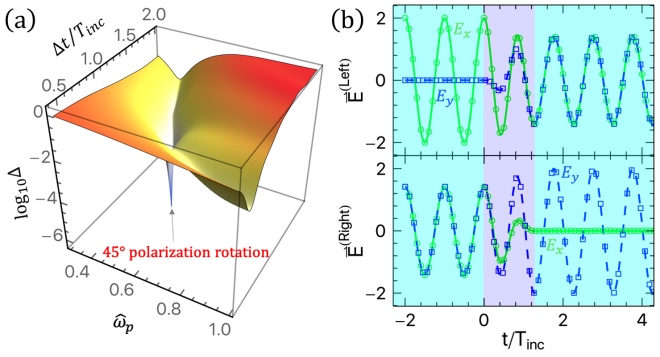

FIG. 3. (a) $\log_{10}\Delta$ as a function of the normalized plasma frequency $\hat{\omega}_p$ of the temporal magnetoplasma slab in Fig. 1(b) and its thickness Δt (in units of T_{inc}). (b) Time-dependent evolution of the electric field components at $z = 0$ in the case of left (upper panel) and right incidence (lower panel) for the demonstration of a perfect 45° Faraday rotator occurring at $\hat{\omega}_p \approx 0.535$ and $\Delta t/T_{inc} \approx 1.28$, consistent with the minimum in panel (a). The theoretical results (solid and dashed lines) have been verified by FDTD simulations (symbols), and the colored backgrounds indicate time-varied material properties. For both subfigures, $\hat{\omega}_c = 0.7$.

with $E_x = E_y$ as it travels through the temporal slab in the forward direction [see upper panel]. In turn, a wave traveling in the backward direction with polarization state $E_x = E_y$, is converted to vertical polarization, i.e., $E_x = 0$, after traveling through the temporal slab (see lower panel) [46], yielding nonreciprocity and the time analog of a Faraday polarization rotator without the need for spatial interfaces [57]. Quite interestingly, in both scenarios the time-reflected waves after the temporal slab are very small at the optimal point (see also animations in Ref. [46]), although counterpropagating waves at *different frequencies* exist within the temporal slab. In addition, at this optimal condition the total power flow is conserved, and thus the power of the impinging waves is fully transferred to the transmitted waves.

Conclusions.—In this Letter, we have introduced the concept of nonreciprocity for temporal interfaces. We demonstrated the possibility of realizing nonreciprocal polarization conversion in a dispersive temporal magnetoplasma slab, and devised a temporal Faraday rotator. Quite different from conventional nonreciprocal devices typically suited for a narrow frequency range, our temporal slab inherently operates through the interference of multiple counter-propagating plane waves at different frequencies. As confirmed by the good agreement between our theoretical predictions referring to unbounded media and FDTD simulations for finite wave trains, our results hold as long as the material is switched uniformly within the volume occupied by the traveling signals. We envision interesting opportunities arising as we extend this concept to higher spatial dimensions, as well as to finite systems supporting resonant phenomena and in the presence of non-Hermitian features [22].

This work was supported by the Simons Foundation and the Air Force Office of Scientific Research MURI program.

*These authors contributed equally to this work.
†Corresponding author.
aalu@gc.cuny.edu

[1] N. Engheta, Metamaterials with high degrees of freedom: Space, time, and more, Nanophotonics **10**, 639 (2021).
[2] V. Bacot, M. Labousse, A. Eddi, M. Fink, and E. Fort, Time reversal and holography with spacetime transformations, Nat. Phys. **12**, 972 (2016).
[3] A. V. Maslov and M. I. Bakunov, Temporal scattering of a graphene plasmon by a rapid carrier density decrease, Optica **5**, 1508 (2018).
[4] E. Lustig, Y. Sharabi, and M. Segev, Topological aspects of photonic time crystals, Optica **5**, 1390 (2018).
[5] A. V. Shirokova, A. V. Maslov, and M. I. Bakunov, Scattering of surface plasmons on graphene by abrupt free-carrier generation, Phys. Rev. B **100**, 045424 (2019).
[6] M. R. Shcherbakov, K. Werner, Z. Fan, N. Talisa, E. Chowdhury, and G. Shvets, Photon acceleration and tunable broadband harmonics generation in nonlinear time-dependent metasurfaces, Nat. Commun. **10**, 1345 (2019).
[7] D. Ramaccia, A. Toscano, and F. Bilotti, Light propagation through metamaterial temporal slabs: Reflection, refraction, and special cases, Opt. Lett. **45**, 5836 (2020).
[8] Y. Zhou, M. Z. Alam, M. Karimi, J. Upham, O. Reshef, C. Liu, A. E. Willner, and R. W. Boyd, Broadband frequency translation through time refraction in an epsilon-near-zero material, Nat. Commun. **11**, 2180 (2020).
[9] V. Pacheco-Peña and N. Engheta, Antireflection temporal coatings, Optica **7**, 323 (2020).
[10] D. Ramaccia, A. Alù, A. Toscano, and F. Bilotti, Temporal multilayer structures for designing higher-order transfer functions using time-varying metamaterials, Appl. Phys. Lett. **118**, 101901 (2021).
[11] J. Xu, W. Mai, and D. H. Werner, Complete polarization conversion using anisotropic temporal slabs, Opt. Lett. **46**, 1373 (2021).
[12] Y. Sharabi, E. Lustig, and M. Segev, Disordered Photonic Time Crystals, Phys. Rev. Lett. **126**, 163902 (2021).
[13] R. Carminal, H. Chen, R. Pierrat, and B. Shapiro, Universal Statistics of Waves in a Random Time-Varying Medium, Phys. Rev. Lett. **127**, 094101 (2021).
[14] V. Pacheco-Peña and N. Engheta, Temporal metamaterials with gain and loss, arXiv:2108.01007.
[15] E. Galiffi, R. Tirole, S. Yin, H. Li, S. Vezzoli, P. A. Huidobro, M. G. Silveirinha, R. Sapienza, A. Alù, and J. B. Pendry, Photonics of time-varying media, Adv. Opt. Photonics **4**, 014002 (2022).
[16] A. Akbarzadeh, N. Chamanara, and C. Caloz, Inverse prism based on temporal discontinuity and spatial dispersion, Opt. Lett. **43**, 3297 (2018).
[17] V. Pacheco-Peña and N. Engheta, Temporal aiming, Light Sci. Appl. **9**, 129 (2020).

[18] A. Shlivinski and Y. Hadad, Beyond the Bode-Fano Bound: Wideband Impedance Matching for Short Pulses Using Temporal Switching of Transmission-Line Parameters, Phys. Rev. Lett. **121**, 204301 (2018).
[19] H. Li and A. Alù, Temporal switching to extend the bandwidth of thin absorbers, Optica **8**, 24 (2021).
[20] C. Firestein, A. Shlivinski, and Y. Hadad, Absorption and Scattering by a Temporally Switched Lossy Layer: Going beyond the Rozanov Bound, Phys. Rev. Applied **17**, 014017 (2022).
[21] Y. Mazor, M. Cotrufo, and A. Alù, Unitary Excitation Transfer between Coupled Cavities Using Temporal Switching, Phys. Rev. Lett. **127**, 013902 (2021).
[22] H. Li, S. Yin, E. Galiffi, and A. Alù, Temporal Parity-Time Symmetry for Extreme Energy Transformations, Phys. Rev. Lett. **127**, 153903 (2021).
[23] C. Caloz, A. Alù, S. Tretyakov, D. Sounas, K. Achouri, and Z.-L. Deck-Léger, Electromagnetic Nonreciprocity, Phys. Rev. Applied **10**, 047001 (2018).
[24] N. Bender, S. Factor, J. D. Bodyfelt, H. Ramezani, D. N. Christodoulides, F. M. Ellis, and T. Kottos, Observation of Asymmetric Transport in Structures with Active Nonlinearities, Phys. Rev. Lett. **110**, 234101 (2013).
[25] Y. Yu, Y. Chen, H. Hu, W. Xue, K. Yvind, and J. Mork, Nonreciprocal transmission in a nonlinear photonic-crystal Fano structure with broken symmetry, Laser Photonics Rev. **9**, 241 (2015).
[26] D. L. Sounas, J. Soric, and A. Alù, Broadband passive isolators based on coupled nonlinear resonances, Nat. Electron. **1**, 113 (2018).
[27] M. Cotrufo, S. A. Mann, H. Moussa, and A. Alù, Nonlinearity-induced nonreciprocity—Part I, IEEE Trans. Microwave Theory Tech. **69**, 3569 (2021).
[28] M. Cotrufo, S. A. Mann, H. Moussa, and A. Alù, Nonlinearity-induced nonreciprocity—Part II, IEEE Trans. Microwave Theory Tech. **69**, 3584 (2021).
[29] L. Bi, J. Hu, P. Jiang, D. H. Kim, G. F. Dionne, L. C. Kimerling, and C. A. Ross, On-chip optical isolation in monolithically integrated non-reciprocal optical resonators, Nat. Photonics **5**, 758 (2011).
[30] Y. Zhang, Q. Du, C. Wang, T. Fakhrul, S. Liu, L. Deng, D. Huang, P. Pintus, J. Bowers, C. A. Ross, J. Hu, and L. Bi, Monolithic integration of broadband optical isolators for polarization-diverse silicon photonics, Optica **6**, 473 (2019).
[31] M. I. Abdelrahman and F. Monticone, Broadband and giant nonreciprocity at the subwavelength scale in magnetoplasmonic materials, Phys. Rev. B **102**, 155420 (2020).
[32] Z. Yu and S. Fan, Complete optical isolation created by indirect interband photonic transitions, Nat. Photonics **3**, 91 (2009).
[33] H. Lira, Z. Yu, S. Fan, and M. Lipson, Electrically Driven Nonreciprocity Induced by Interband Photonic Transition on a Silicon Chip, Phys. Rev. Lett. **109**, 033901 (2012).
[34] N. A. Estep, D. L. Sounas, J. Soric, and A. Alù, Magnetic-free non-reciprocity and isolation based on parametrically modulated coupled-resonator loops, Nat. Phys. **10**, 923 (2014).
[35] F. Ruesink, M.-A. Miri, A. Alù, and E. Verhagen, Nonreciprocity and magnetic-free isolation based on optomechanical interactions, Nat. Commun. **7**, 13662 (2016).
[36] S. Taravati and C. Caloz, Mixer-duplexer-antenna leaky-wave system based on periodic space-time modulation, IEEE Trans. Antennas Propag. **65**, 442 (2017).
[37] J. Kim, S. Kim, and G. Bahl, Complete linear optical isolation at the microscale with ultralow loss, Sci. Rep. **7**, 1647 (2017).
[38] D. Sounas and A. Alù, Non-reciprocal photonics based on time modulation, Nat. Photonics **11**, 774 (2017).
[39] H. Li, T. Kottos, and B. Shapiro, Floquet-network theory of nonreciprocal transport, Phys. Rev. Applied **9**, 044031 (2018).
[40] E. Galiffi, P. A. Huidobro, and J. B. Pendry, Broadband Nonreciprocal Amplification in Luminal Metamaterials, Phys. Rev. Lett. **123**, 206101 (2019).
[41] X. Wang, G. Ptitcyn, V. S. Asadchy, A. Díaz-Rubio, M. S. Mirmoosa, S. Fan, and S. A. Tretyakov, Nonreciprocity in Bianisotropic Systems with Uniform Time Modulation, Phys. Rev. Lett. **125**, 266102 (2020).
[42] V. S. Asadchy, M. S. Mirmoosa, A. Díaz-Rubio, S. Fan, and S. A. Tretyakov, Tutorial on electromagnetic nonreciprocity and its origins, Proc. IEEE **108**, 1684 (2020).
[43] A. Ishimaru, *Electromagnetic Wave Propagation, Radiation, and Scattering* (John Wiley & Sons, New Jersey, 2017).
[44] See also Ref. [45] for targeting nonlinear responses in the case of large amplitude excitations.
[45] P. Gibbon, *Short Pulse Laser Interactions with Matter* (Imperial College Press, London, 2005).
[46] See Supplemental Material at http://link.aps.org/supplemental/10.1103/PhysRevLett.128.173901 for detailed derivations, effects of transition times of the switching events on the 45° temporal Faraday polarization rotator, and movies of the time evolution associated with Figs. 2 and 3.
[47] D. K. Kalluri, Conversion of a whistler wave into a controllable helical wiggler magnetic field, J. Appl. Phys. **79**, 6770 (1996).
[48] J. Gratus, R. Seviour, P. Kinsler, and D. A. Jaroszynski, Temporal boundaries in electromagnetic materials, New J. Phys. **23**, 083032 (2021).
[49] D. K. Kalluri, *Electromagnetics of Time Varying Complex Media: Frequency and Polarization Transformer* (CRC Press, Boca Raton, 2010).
[50] D. K. Kalluri, Effect of switching a magnetoplasma medium on a traveling wave: Longitudinal propagation, IEEE Trans. Antennas Propag. **37**, 1638 (1989).
[51] D. K. Kalluri and V. R. Goteti, Damping rates of waves in a switched magnetoplasma medium: Longitudinal propagation, IEEE Trans. Plasma Sci. **18**, 797 (1990).
[52] M. I. Bakunov and A. V. Maslov, Reflection and transmission of electromagnetic waves at a temporal boundary: Comment, Opt. Lett. **39**, 6029 (2014).
[53] It is interesting to compare this result with Ref. [54] where ultrashort laser pulses split in plasma without changing frequency due to large spatial Faraday phenomena. Quite differently, our temporal Faraday effect discussed here relies on counterpropagating waves overlapping in space after switching.
[54] S. Weng, Q. Zhao, Z. Sheng, W. Yu, S. Luan, M. Chen, L. Yu, M. Murakami, W. B. Mori, and J. Zhang, Extreme case of Faraday effect: Magnetic splitting of ultrashort laser pulses in plasmas, Optica **4**, 1086 (2017).
[55] Indeed, the appearance of complex conjugation becomes obvious when considering wave propagation within one

temporal slab of thickness Δt in a reciprocal medium [22]. In this case, the time-dependent amplitudes of forward and backward waves are simply proportional to $e^{j\omega t}$ and $e^{-j\omega^* t}$, respectively, and thus the transmission amplitudes are $t_{L\to R} = t^*_{R\to L} = e^{j\omega\Delta t}$.

[56] Around this point, the dependence of $\log_{10}\Delta$ on $\hat{\omega}_c$ and Δt when fixing $\hat{\omega}_p \approx 0.535$ exhibits a qualitatively similar surface as Fig. 3(a). Besides, the position of this optimal point on $\hat{\omega}_p - \Delta t$ plane [see Fig. 3(a)] can be controlled by the specific value of $\hat{\omega}_c$.

[57] J. Y. Chin, T. Steinle, T. Wehlus, D. Dregely, T. Weiss, V. I. Belotelov, B. Stritzker, and H. Giessen, Nonreciprocal plasmonics enables giant enhancement of thin-film Faraday rotation, Nat. Commun. **4**, 1599 (2013).